

## ARTICLES

## Connection between Proton Abnormal Conductivity in Water and Dielectric Relaxation Time

Boiko Cohen and Dan Huppert\*

Raymond and Beverly Sackler Faculty of Exact Sciences, School of Chemistry, Tel Aviv University, Tel Aviv 69978, Israel

Received: May 2, 2002; In Final Form: February 24, 2003

High proton conductivity in aqueous solutions has been known for a long time and is attributed to the Grotthus mechanism. In this study, we calculated the proton-transfer rate constant associated with prototropic mobility in water as a function of temperature. We found a strong correlation between the proton-transfer rate constant at low temperatures,  $T < 290$  K, and the dielectric relaxation time. The model that we used to calculate the proton-transfer rate constant is based on diffusive propagation of the solvent configuration along a generalized solvent coordinate from the reactant potential surface toward the crossing point with the product potential surface. The proton transfer occurs at the crossing point, and the rate is calculated by a sink term placed at the crossing point. The sink term includes the solvent velocity and the Landau–Zener transmission coefficient. Both the diffusion constant and the Landau–Zener transmission coefficient depend on the dielectric relaxation of the solvent. The calculations are compared with the proton mobility data and an interpolation expression that bridges the nonadiabatic limit and the solvent-controlled limit.

## Introduction

The abnormally high conductivity of acids and bases in aqueous solutions was first observed over 150 years ago. Over the last few decades, the field of abnormal proton conductivity has been investigated by several authors.<sup>1–3</sup> At 25 °C, the equivalent conductivity at infinite dilution,  $\lambda^0$ , is 349.8 for  $\text{H}_3\text{O}^+$  and 198.1 for  $\text{OH}^-$ . These values should be compared to values of 37.5, 50.1, and 73.6 for  $\text{Li}^+$ ,  $\text{Na}^+$ , and  $\text{K}^+$ , respectively, and 76.4 and 68.1 for  $\text{Cl}^-$  and  $\text{ClO}_4^-$ , respectively, all values in  $\text{cm}^2 \Omega^{-1} \text{equiv}^{-1}$ .

Another important difference between proton mobility and ion conductivity is the unusual temperature dependence. The alkaline cation conductivity in water has an Arrhenius behavior (constant activation energy,  $E_a$ ), while the temperature dependence of the proton conductivity in water has a non-Arrhenius behavior. The activation energy of the latter is smaller at higher temperature.  $E_a$  of the regular ion conductance in water is about 16 kJ/mol, while the activation energy of the abnormal proton conductance changes from about 32 kJ/mol in supercooled water at 244 K to about 4 kJ/mol at the boiling point 373 K.<sup>4</sup>

In textbooks, high proton conductivity is usually attributed to the Grotthus mechanism.<sup>5</sup> As a general mechanism of conduction in ionic solutions, Grotthus<sup>6</sup> suggested, in 1806, a chain mechanism for the transfer of charge along a chain of particles. The resemblance of this mechanism to the proton-transfer case is formal rather than physically analogous. Two classes of proton-transport phenomena are recognized in liquid water: “ordinary” mass diffusion according to Stokes law and

the “abnormal” proton mobility, which we shall deal with in this study. The value of the abnormal proton conductivity is obtained by subtracting the Stokes mass diffusion contribution to the conductance from the total conductance,  $\lambda_{\text{H}^+} = \lambda_{\text{H}^+}^{\text{ab}} + \lambda_{\text{H}^+}^{\text{St}}$ , where  $\lambda_{\text{H}^+}^{\text{ab}}$  and  $\lambda_{\text{H}^+}^{\text{St}}$  are the abnormal and Stokes equivalent conductivity, respectively. Using a random walk description, we characterize the abnormal proton mobility in water by a hopping time,  $\tau_p$ , of about 1.5 ps at room temperature, as deduced from NMR line-narrowing investigations.<sup>7–9</sup> This time scale reproduces the “abnormal” proton mobility with a hopping length,  $l_p$ , of 2.5–2.6 Å, the O–O distance in  $\text{H}_2\text{O}$ .

$$\tau_p = l_p^2 / (6D_{\text{H}^+}^{\text{ab}}) \quad D_{\text{H}^+}^{\text{ab}} = k_B T \lambda_{\text{H}^+}^{\text{ab}} / (z^2 F^2) \quad (1)$$

where  $z$  is the protic charge,  $F$  is Faraday’s constant,  $D_{\text{H}^+}^{\text{ab}}$  is the contribution of the abnormal proton mobility to the proton diffusion constant, and  $l_p = 2.55$  Å.<sup>4</sup>

Since the work of Bernal and Fowler,<sup>10</sup> the rate-determining step of prototropic mobility is believed to be connected to single-water rotation.<sup>1,4,11</sup> Traditionally the dielectric relaxation time,  $\tau_D$ , of a liquid is associated with molecular rotation time. Dielectric relaxation and self-diffusion are slower than the hopping time,  $\tau_p$ , related to the abnormal conductivity and show stronger temperature dependence than  $\tau_p$ . From  $\lambda_{\text{H}^+} = \lambda_{\text{H}^+}^{\text{ab}} + \lambda_{\text{H}^+}^{\text{St}}$ , it would be hard to connect the prototropic mobility with the time scale of  $\tau_D$ .

Several theories suggest that the microscopic relaxation time is some fraction of  $\tau_D$ . Powels–Glarum model<sup>12</sup> implies that, for water, the microscopic reorientation time is  $2\tau_D/3$ . While such corrections adjust the time scales of  $\tau_p$  and  $\tau_D$  to better agree with experimental data, they do not completely eliminate

\* To whom correspondence should be addressed. E-mail: huppert@tulip.tau.ac.il. Fax/phone: 972-3-6407012.

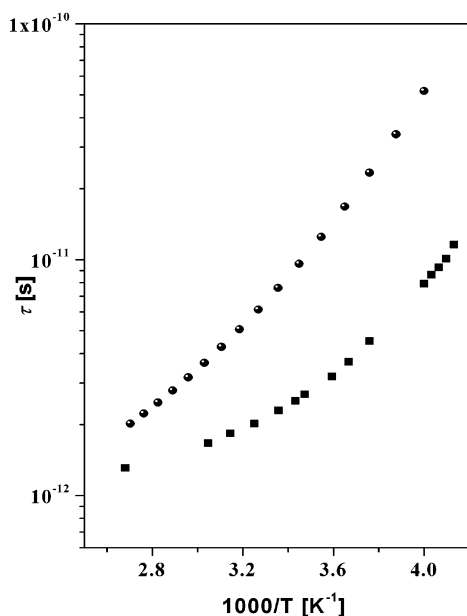


**Figure 1.** Proton-hopping times,  $\tau_p$  (■), as a function of  $1/T$ , calculated from proton mobility data,  $\lambda_{H^+}$ , according to eq 2, along with the dielectric relaxation times,  $\tau_D$  (●).

the discrepancy. Agmon<sup>4</sup> used eq 2 to calculate the hopping time,  $\tau_p$

$$\tau_p = \frac{3}{2} \left[ \frac{l_p^2}{6(k_B T \lambda_{H^+} / (z^2 F^2) - D_S)} \right] \quad (2)$$

The “abnormal” part of the proton’s diffusion coefficient is obtained by subtracting from it the water self-diffusion coefficient,  $D_S$ .<sup>13</sup> The factor  $3/2$  corresponds to the Powel–Glarm correction. Figure 1 shows proton-hopping times,  $\tau_p$ , calculated from proton mobility data,<sup>14,15</sup>  $\lambda_{H^+}$ , according to eq 2.

While  $\tau_p$  agrees with the NMR hopping times, the discrepancy between it and  $\tau_D$  remains large, particularly when compared with the close agreement between  $\eta$  and  $\tau_D$ . Moreover, the temperature dependence of the two processes is different. The activation energy of  $\tau_p$  is smaller than  $\tau_D$  by more than 4 kJ/mol. In this study, we wish to connect  $\tau_p$  and  $\tau_D$  and explain how  $\tau_D$ , which serves as the characteristic solvent motion time scale, influences  $\tau_p$ .

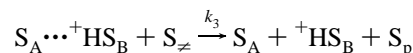
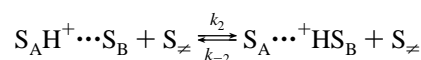
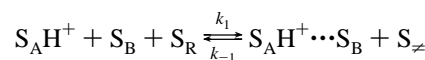
In a recent paper,<sup>16</sup> we calculated the proton-transfer rate constant from a super photoacid, 5,8-dicyano-2-naphthol (DCN2), to protic solvents such as methanol and glycerol as a function of temperature. The temperature dependence of the proton-transfer rate constant shows unusual behavior. Similar to the abnormal proton conductivity in water, the activation energy is not constant. At high temperatures, the activation energy is low, while at low temperatures, it is high. Also we found that the inverse of the proton-transfer rate constant at low temperature has a value similar to  $\tau_D$ . Previously,<sup>17–20</sup> we found that the temperature dependence of the proton-transfer rate constant from several photoacids to solvent is explained as a continuous transition from nonadiabatic to solvent-controlled limits. In the nonadiabatic limit, the rate-determining step in the proton-transfer rate is the proton tunneling from the proton donor (the acid) to the proton acceptor (a hydrogen-bonded solvent molecule). In the solvent-controlled limit, the solvent motion, to reach the generalized curve-crossing solvent configuration, is the rate-limiting step of the proton-transfer reaction. We found that the characteristic time for the solvent motion,  $\tau_S$ , is a fraction

of the dielectric relaxation time,  $\tau_S = \tau_D/b$ , where  $b$  is an empirical factor. For methanol,  $b$  is about 2.  $\tau_S$  is longer than the longitudinal dielectric relaxation time,  $\tau_L = (\epsilon_\infty/\epsilon_S)\tau_D$ , where  $\epsilon_\infty$  and  $\epsilon_S$  are the high-frequency and static dielectric constants, respectively.

The abnormal proton conductivity in water arises from the efficient reaction of proton transfer from  $H_3O^+$ , or larger hydrogen-bonded complexes such as  $H_9O_4^+$  (Eigen’s complex)<sup>21</sup> or  $H_5O_2^+$  (the Zundel’s dimer),<sup>22</sup> to a nearby water molecule or larger hydrogen-bonded complexes. Agmon<sup>11</sup> suggested that the molecular mechanism behind prototropic mobility involves a periodic series of isomerizations between  $H_9O_4^+$  and  $H_5O_2^+$ , the first triggered by the hydrogen-bond cleavage of a second-shell water molecule and the second by the reverse hydrogen-bond formation process.

Our calculation of the proton-transfer rate associated with the abnormal conductivity is based on the nonadiabatic proton-transfer theory developed by Kuznetsov and his colleagues.<sup>23–27</sup> The theory is very similar to the nonadiabatic electron transfer in its treatment of the involvement of the solvent. The fundamental assumption is that when a barrier is encountered in the proton-transfer coordinate, the proton tunnels through the barrier, thus leading to a nonadiabatic process. In the Kuznetsov model, when the polar solvent is equilibrated to the reactant, the proton will not be transferred because of an energy mismatch in the reactant and product states. Upon a solvent fluctuation, the energy of the reactant and product states becomes equal, and it is in this solvent configuration that the proton tunnels from the reactant well to the product well. Finally, upon solvent relaxation, the product state is formed.

If the pretunneling and posttunneling configurations are regarded as real transient intermediates, the process can be described by a set of chemical equations:<sup>28</sup>



where  $S_A H^+$  is the hydronium ion,  $H_3O^+$  or a larger hydrogen-bonded complex.  $S_B$  is a single water molecule or a larger hydrogen-bonded complex to which the proton is transferred,  $S_R$  is the solvent configuration to stabilize the reactants, and  $S_p$  is the solvent configuration of the products.  $S_\neq$  is the solvent configuration to equally stabilize  $S_A H^+ \cdots S_B$  and  $S_A \cdots H S_B$ .

The model that we used to calculate the proton-transfer rate constant is based on the diffusive propagation of the population of the reactant,  $S_A H^+ + S_B$ , along a generalized solvent coordinate initially from the equilibrium configuration of the reactant potential surface toward the crossing point of the product potential surface. The proton transfer occurs at the crossing point, and the rate is calculated by a sink term placed at the crossing point. The sink term includes the solvent velocity and the Landau–Zener transmission coefficient. Both the diffusion constant and the Landau–Zener transmission coefficient depend on the dielectric relaxation of the solvent, which in turn depends on the water temperature.

In the present work, we calculate the proton-transfer rate constant associated with the abnormal conductivity of an excess proton in water as a function of  $1/T$  (from supercooled water at  $\sim 244$  K up to the boiling point at 373 K). The calculation is based on the Landau–Zener curve-crossing formulation and its

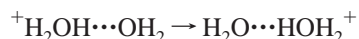
relation to the water characteristic time scale, the water dielectric relaxation time. We find very good correlation between our calculations and the experimental results.

The calculation suggests that at high temperatures,  $T > 290$  K, the abnormal proton conductance can be described by a proton-transfer reaction in the nonadiabatic limit. In that limit, proton tunneling is the rate-limiting step. For supercooled water, the proton-transfer rate constant is determined by both the tunneling rate and the solvent motion.

### Modeling of the Proton Abnormal Conductivity

The prototropic conductivity in water arises from a reaction of proton transfer from  $\text{H}_3\text{O}^+$  or larger hydrogen-bonded complexes to a nearby water molecule or larger hydrogen-bonded complexes. Agmon<sup>11</sup> suggested that the molecular mechanism behind prototropic mobility involves a periodic series of isomerizations between  $\text{H}_9\text{O}_4^+$  and  $\text{H}_5\text{O}_2^+$ , the first triggered by hydrogen-bond cleavage of a second-shell water molecule and the second by the reverse hydrogen-bond formation process ("Moses mechanism"). Recently, Parinello and co-workers<sup>29–31</sup> looked at the nature of the hydrated excess proton in water using ab initio simulations. They found that the hydrated proton forms a defect in the hydrogen-bonded network with both  $\text{H}_9\text{O}_4^+$  and  $\text{H}_5\text{O}_2^+$  dimer structures and the rate of proton diffusion is determined by thermally induced hydrogen-bond breaking in the second solvation shell. For simplicity, we shall describe the process by a conservative traditional scheme:

Scheme 1



The reactant is an intermolecular hydrogen-bonded complex between  $\text{H}_3\text{O}^+$  and a water molecule, which serves as a base, characterized by a hydrogen bond to  $\text{H}_3\text{O}^+$  and other solvent molecules. In water, this specific water molecule, denoted as  $\text{S}_B$ , has three hydrogen bonds to three water molecules. To form the product,  $\text{HS}_B^+$ , one hydrogen bond of  $\text{S}_B$  to a water molecule must be broken. Thus, relatively long-range reorganization of the hydrogen-bond network takes place upon proton transfer to the water. This complex rearrangement to accommodate the product is probably the reason for the relatively slow water-generalized configuration motion, which corresponds to a low-frequency component in the water dielectric spectrum. Its time constant,  $\tau_S$ , is shorter than the dielectric relaxation time,  $\tau_D$ , but longer than  $\tau_L$ .

According to Kuznetsov and co-workers,<sup>23–27</sup> Borgis and Hynes,<sup>32</sup> Bernstein and co-workers,<sup>33</sup> and Syage,<sup>34</sup> a second important coordinate should be taken into account. This second coordinate is the distance between the two heavy atoms,  $\text{O}-\text{H}\cdots\text{O}$  in our case. This distance is modulated by a low-frequency vibrational mode,  $Q$ .<sup>32,33</sup> The proton tunnels through the barrier from the reactant well to the product well via the assistance of the low-frequency,  $Q$ , mode whenever the solvent configuration equalizes the energies of the reactant and the product. The reaction rate constant for the proton transfer of the proton abnormal conductivity is given by  $k_{\text{PT}}(T) = 1/\tau_p(T)$ .

Figure 2a shows the temperature dependence of the proton-transfer reaction rate constant,  $k_{\text{PT}}$ , calculated from the  $\tau_p$  data shown in Figure 1, as a function of  $1/T$ , and Figure 2b shows the activation energy for the process.

In a transition-state theory form, the reaction rate constant,  $k$ , is expressed as the average one-way flux along the solvent coordinate through the crossing point  $S^\ddagger$  of the two free-energy surfaces with the inclusion of a transmission coefficient,  $\kappa$ ,

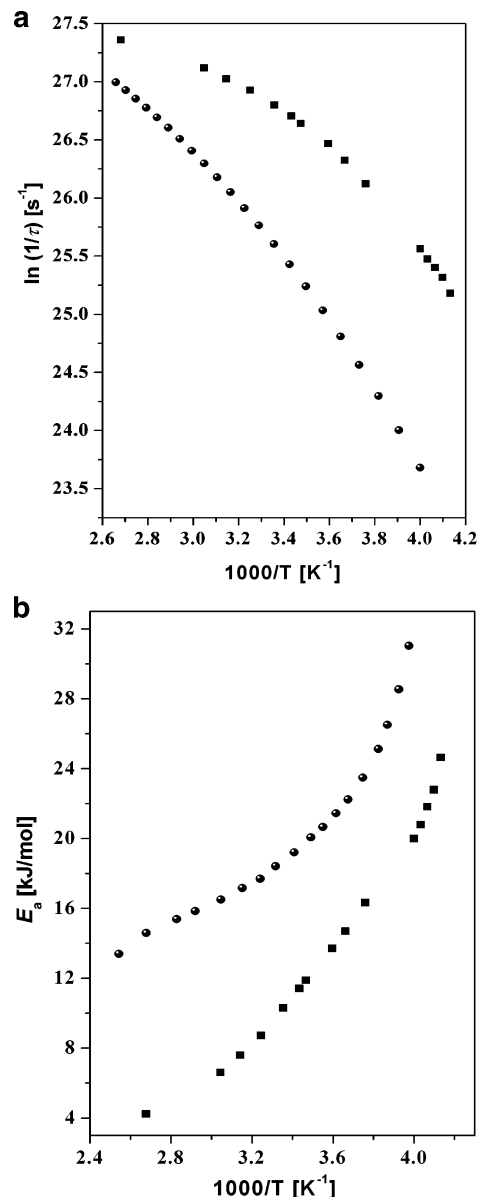


**Figure 2.** Temperature dependence of (a) the proton-transfer reaction rate constant,  $k_{\text{PT}}$  (■), calculated from the  $\tau_p$  data shown in Figure 1, along with the inverse of the dielectric relaxation time,  $1/\tau_D$  (●), and (b) activation energies of the proton transfer (■) and the dielectric relaxation (●) processes.

giving the probability of a successful curve crossing:

$$k = \langle \dot{S} \Theta(\dot{S}) \delta(S - S^\ddagger) \kappa(\dot{S}, S^\ddagger) \rangle_{\text{R}} \quad (3)$$

where  $S$  is the generalized solvent coordinate,  $\dot{S}$  the solvent velocity, and  $\Theta(\dot{S})$  the step function. The brackets denote averaging over the classical solvent distribution normalized by the partition function of the solvent.

To find the appropriate nonadiabatic transmission coefficient,  $\kappa$ , for use in this equation, Borgis and Hynes<sup>32</sup> used the general Landau–Zener (LZ) transmission coefficient,  $\kappa_{\text{LZ}}$ , adapted for the present problem. The LZ factor, appropriate for a positive velocity approach to the crossing point, is

$$\kappa_{\text{LZ}} = [1 - 1/2 \exp(-\gamma)]^{-1} [1 - \exp(-\gamma)] \quad (4)$$

where

$$\gamma = \frac{2\pi|V|^2}{\hbar\Delta F\dot{S}} = \frac{2\pi|V|^2}{\hbar k_S\dot{S}} \quad (5)$$

is the adiabaticity parameter. The expression for the transmission coefficient  $\kappa_{LZ}$  includes multiple passage effects on the transition probability.  $V$  is the coupling matrix element between the reactant and the product, and  $\Delta F$  is the slope difference of the diabatic potentials of mean force at the crossing point,  $\Delta F = k_S$ , where  $k_S$  is the parabolic potential surface force constant. When  $\gamma \ll 1$ , one obtains the nonadiabatic limit result

$$\kappa_{LZ} \cong 2\gamma \quad (6)$$

leading to

$$k_{NA} = \frac{2\pi}{\hbar}|V|^2 \left(\frac{\beta}{4\pi E_S}\right)^{1/2} \exp(-\beta\Delta G_{NA}^\ddagger) \quad (7)$$

in which  $\Delta G^\ddagger$  is the Marcus activation free energy

$$\Delta G_{NA}^\ddagger = \frac{1}{4E_S}(E_S + \Delta G)^\ddagger \quad (8)$$

In eq 7,  $\beta = k_B T$  and  $E_S$  is the solvent reorganization energy.

The adiabaticity parameter,  $\gamma$  (see eq 5), depends on three parameters, the potential surfaces curvature ( $\Delta F$ ), the coupling ( $|V|^2$ ), and the velocity in the vicinity of crossing, ( $\dot{S}$ ).  $|V|^2$  is independent of temperature. The solvent velocity,  $\dot{S}$ , on the other hand, strongly depends on the temperature. In our previous papers,<sup>17–20</sup> we suggested that  $\dot{S}$  is related to the slow components of the solvent dielectric relaxation. We infer that  $\dot{S} = b/\tau_D$ , where  $\tau_D$  is the solvent dielectric relaxation time and  $b$  is an empirical factor, dependent on the specific protic solvent, and its value is between 1 and 4 for the proton-transfer reaction from a photoacid to several alcohols.

The adiabaticity parameter,  $\gamma$ , is small at high temperatures and large at low temperatures. For the proton-transfer reaction from a photoacid to alcohols, we found that the value of  $\gamma$  as a function of the temperature increases smoothly from a value close to 0, that is,  $\gamma \ll 1$  (the nonadiabatic limit) to a value  $\gamma \gg 1$  (the adiabatic limit).

In the adiabatic limit,  $V \gg k_B T$  and  $\kappa_{LZ} \approx 1$ , the adiabatic rate expression is

$$k_{AD} = (\omega_s/2\pi) \exp(-\beta\Delta G_{AD}^\ddagger) \quad (9)$$

where  $\omega_s$  is the solvent high frequency and  $\Delta G_{AD}^\ddagger \cong \Delta G_{NA}^\ddagger - V$  is the free energy of activation.

Another physical limit is realized when  $V \leq k_B T$  and the interaction with the environment is strong enough. In this *solvent-controlled limit*, the rate is inversely proportional to the solvent relaxation time (friction) and independent of the coupling,  $V$ . Rips and Jortner<sup>35,36</sup> derived an expression for the resonant electron-transfer rate in the solvent-controlled limit.

$$k_{SC}^{ET} = \frac{1}{\tau_L} \left(\frac{E_S}{16\pi k_B T}\right)^{1/2} \exp(-\beta\Delta G_{NA}^\ddagger) \quad (10)$$

The preexponent in the solvent-controlled limit depends on the solvent's dynamical properties. For the nonresonance cases, the prefactor in the rate expression (eq 10) only changes by about 20%.

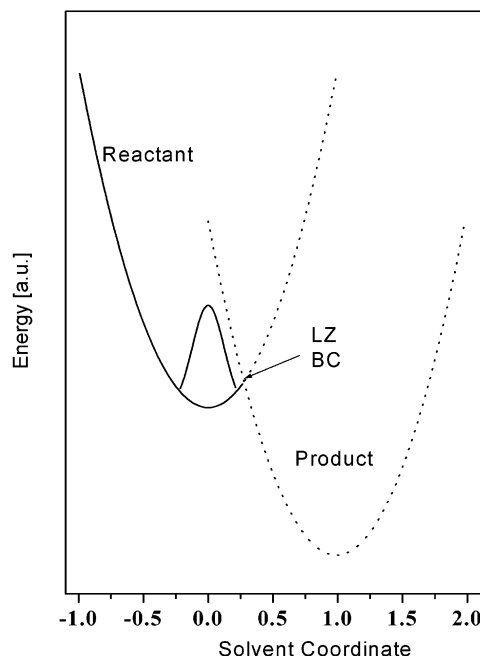


**Figure 3.** Schematic representation of the model for the calculation of the abnormal proton conductance. LZBC denotes the Landau–Zener boundary condition at the crossing point between the diabatic potential surfaces (see text) of the proton donor (reactant) and proton acceptor (product).

In alcohols, at low temperatures, we found that the preexponential factor in the solvent-controlled limit is related to the slowest component of the dielectric relaxation time.<sup>17–20</sup> We also found that the temperature dependence of the proton-transfer rate constant can be explained as a continuous transition from the nonadiabatic limit at high temperature to the solvent-controlled limit at low temperature.

Figure 3 schematically shows the model for the calculation of the abnormal proton conductance. We use two crossing parabolic potential surfaces representing the free energy of the reactant and product along the solvent coordinate. For numerical calculation purposes, we focus our attention on the reactant single-well parabolic potential surface in the generalized solvent coordinate. The numerical calculation is based on the diffusive propagation of the solvent generalized coordinate from the equilibrium position of the reactant well to the crossing point. We solve the Debye–Smoluchowski equation (DSE) for the specific problem. The probability density function,  $\rho(S,t)$ , to find a solvent configuration,  $S$ , along the generalized solvent coordinate at time  $t$  obeys the DSE<sup>37–39</sup>

$$\frac{\partial \rho(S,t)}{\partial t} = D \frac{\partial}{\partial S} e^{-\beta U(S)} \frac{\partial}{\partial S} e^{\beta U(S)} \rho(S,t) \quad (11)$$

where  $D$  is a diffusion constant and  $U(S)$  is the potential surface.

In the numerical calculation, we used

$$U_r(S) = \frac{1}{2}k_S S^2$$

$$U_p(S) = \frac{1}{2}k_S(S - S_p)^2 \quad (12)$$

where  $k_S = 2E_S$  and  $S$  is the generalized and normalized solvent coordinate. In this solvent coordinate, the reactant and product equilibrium positions are at  $S_r = 0$  and  $S_p = 1$ , respectively. For water, we used for the solvent reorganization energy  $E_S = 0.3$  eV. The calculation's initial condition is a thermal equilib-

**TABLE 1: Relevant Parameters for Model Calculations<sup>a</sup>**

	$\tau_D(298\text{K})$ [ps] <sup>b</sup>	$k_0$ [Å/ns] <sup>a,c</sup>	$\gamma'^d$	$D(298\text{K})$ [cm <sup>2</sup> /s] <sup>a,e</sup>	$b^g$
MeOH/	50	$1.35 \times 10^3$	$1.0 \times 10^9$	$3.2 \times 10^{-7}$	2.1
water	8	$1.30 \times 10^3$	$4.5 \times 10^{10}$	$1.25 \times 10^{-5}$	9.2

<sup>a</sup> For calculation with the SSDP program,<sup>40</sup> we used the solvent coordinate in length dimension of Å. Solvent reorganization energy  $E_S = 0.3$  eV. Activation energy  $\Delta G^\ddagger = 0.024$  eV. Crossing point position between the two diabatic potential surfaces,  $S^\ddagger = 0.22$  Å. We placed the minima of the reactant and product potential surfaces at 0 and 1 Å, respectively;  $S_r = 0$  and  $S_p = 1$  Å. <sup>b</sup> Dielectric relaxation time at 298 K. <sup>c</sup>  $k_0$  is a numerical factor, independent of temperature and determined by fitting the numerical solution to the experimental proton-transfer rate constant at high temperatures. <sup>d</sup>  $\gamma'$  is a free adjustable parameter;  $\gamma = \gamma'\tau_S(T)$  (see text). <sup>e</sup> The diffusion coefficient is calculated by  $D = \langle S^2 \rangle / (2\tau_S)$ ,<sup>38</sup>  $\langle S^2 \rangle = 0.16$  is the mean square displacement,  $U(\langle S^2 \rangle^{1/2}) = \sqrt{2E_S k_B T}$  and  $U(S) = \frac{1}{2}k_S S^2$ , where  $k_S = 2E_S$ . <sup>f</sup> Parameters for the proton-transfer rate from DCN2 to methanol are taken from ref 16. <sup>g</sup>  $b$  is a free adjustable parameter;  $\tau_S = \tau_D/b$ .

rium of the probability density function,  $\rho(S)$ , of the solvent coordinate of the reactant and is given by a Gaussian distribution centered at the minimum of the reactant well.

$$\rho_{\text{eq}}(S) = \frac{1}{(2\pi\langle S^2 \rangle)^{1/2}} \exp\left(-\frac{S^2}{2\langle S^2 \rangle}\right) \quad (13)$$

Here,  $\langle S^2 \rangle$  is the mean square displacement, with a Gaussian width, which is determined by the relation  $U(\langle S^2 \rangle^{1/2}) = \sqrt{2E_S k_B T}$ . The diffusion constant,  $D$ , is related to the solvent characteristic time,  $\tau_S = \tau_D/b$ , and the widths of the Gaussian initial distribution,<sup>38</sup>  $D = \langle S^2 \rangle / (2\tau_S)$ . For  $E_S = 0.3$  eV,  $\langle S^2 \rangle \cong 0.16$  at room temperature. We estimate  $\Delta G^\ddagger$  from the temperature dependence of the abnormal conductivity close to the boiling point at 373 K (the nonadiabatic limit). For water, we estimate that  $\Delta G^\ddagger \approx 2.5$  kJ/mol (see Figure 2b). The position of the activation barrier is determined by  $\Delta G^\ddagger = U(S^\ddagger)$  and  $S^\ddagger = 0.22$ .

The next step in the calculation is based upon solving the DSE of a single parabolic potential surface with the relevant initial and boundary conditions. To solve it, we used a graphic program, SSDP (version 2.61) of Krissinel and Agmon,<sup>40</sup> with appropriate boundary condition based on inclusion of the Landau–Zener transmission coefficient,  $\kappa_{LZ}$  (eq 4), in the sink term at the crossing point between the reactant well and the product well. The boundary condition at the crossing point is given by

$$\left. \frac{\partial \rho}{\partial S} \right|_{S=S^\ddagger} = -k_0 \kappa_{LZ} D \rho(S^\ddagger, t) \quad (14)$$

The boundary condition (eq 14) that we chose has similar parameters to the expression for the rate constant expressed in a transition-state theory form (eq 3). The average solvent velocity,  $\langle \dot{S} \rangle$ , is proportional to  $1/\tau_D$ . In eq 14, it is replaced by  $D$ . From the random walk definition,  $D$  is proportional to the random walker average speed.  $k_0$  is a numerical factor, independent of temperature, and is determined by fitting the numerical solution to the experimental proton-transfer rate constant at high temperatures (given in Table 1).  $\kappa_{LZ}$  appears in both expressions.

Finally, the proton-transfer rate constant is obtained from the slope of the plot of  $\ln(\rho)$  versus time. Figure 4 shows the experimental results along with the calculated results using the DSE for the proton-transfer reaction from  $\text{H}_3\text{O}^+$  to water. The relevant parameters for the calculation using the diffusion model

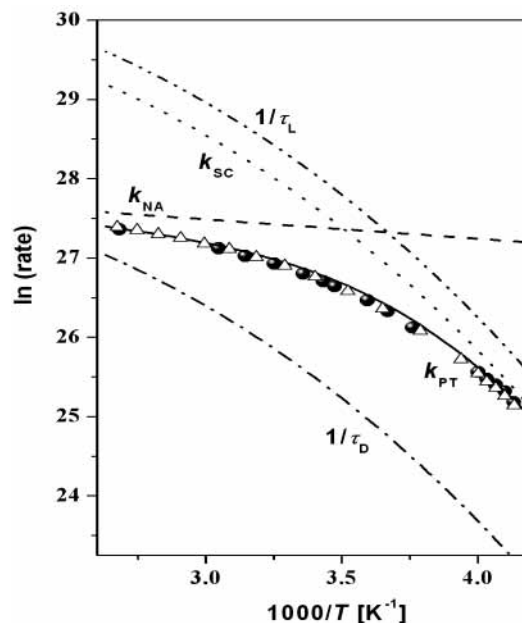


**Figure 4.** The proton-transfer rate deduced from abnormal conductivity, along with the relevant parameters, as a function of  $1/T$ : ( $\Delta$ ) the experimental results; ( $\bullet$ ) the model calculation; (—) the rate calculated by the equation (eq 16); (— · —) the longitudinal dielectric relaxation rate,  $1/\tau_L$ ; (···) the solvent-controlled limit rate constant,  $k_{SC}$ ; (---) the nonadiabatic rate constant  $k_{NA}$ ; (— · —) the inverse dielectric relaxation time  $1/\tau_D$ .

are given in Table 1 with the inclusion of the parameters for our previous calculations of proton transfer from a photoacid to methanol.<sup>16</sup>

The free adjustable parameters in the calculation are  $k_0$ ,  $\gamma'$ , and  $b$ ,

$$\gamma = \gamma'\tau_S(T) \quad (15)$$

From the best fit, we find that  $\gamma' = 4.5 \times 10^{10} \text{ s}^{-1}$ . In the discussion section, we evaluate  $\gamma'$  from eq 7 and the experimental data using some assumptions.  $\tau_S = \tau_D/b$  and  $b = 9.2$  from the best fit to the experimental data for the rate of proton-transfer associated with the abnormal proton conductivity. Figure 5 shows  $\kappa_{LZ}(T)$  as a function of  $1/T$  for the proton-transfer reaction associated with the proton abnormal conductivity in water (circles) and for the proton-transfer reaction from the photoacid DCN2 to methanol (squares). For the abnormal proton conductivity, we find  $\kappa_{LZ} \approx 0.5$  at 244 K, the lowest temperature of available mobility data. At 244 K,  $\tau_S \approx 8$  ps, while  $\tau_D$  at this temperature is about 70 ps.

In our previous papers,<sup>17–20</sup> we used the mean-first-passage expression to bridge between the nonadiabatic limit and the solvent-controlled limit to obtain the rate expression:

$$k_{PT}(T) = \frac{k_{NA}(T)k_{SC}(T)}{k_{NA}(T) + k_{SC}(T)} \quad (16)$$

where  $k_{PT}$  is the overall rate and  $k_{NA}$  and  $k_{SC}$  are given by eqs 7 and 10. We found that this approximation provides a good estimate for the proton-transfer rate constant in the intermediate range in which both the tunneling and the solvent motion influence the reaction rate. In Figure 4, we also see the plots of  $k_{NA}(T)$  and  $k_{SC}(T)$  as a function of  $1/T$ , and the solid line is a calculation based on the mean-first-passage expression (eq 16). The activation energy of both rate constants is low,  $\Delta G^\ddagger = 2.5$  kJ/mol. While  $k_{NA}(T)$  has mild temperature dependence,  $k_{SC}(T)$

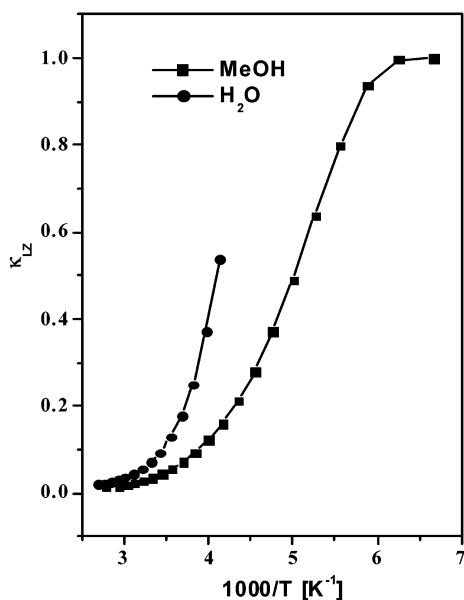


**Figure 5.** The Landau–Zener transmission coefficient,  $\kappa_{LZ}(T)$ , as a function of  $1/T$  for the proton-transfer reaction associated with the proton abnormal conductivity in water (●) and recent calculation (ref 16) for the proton-transfer reaction from the photoacid DCN2 to methanol (■).

has non-Arrhenius temperature behavior and follows approximately  $1/\tau_S(T)$ , where  $\tau_S(T) = \tau_D(T)/b$  (see eq 10).

The model restricts the proton-transfer process to be stepwise. The proton moves to the adjacent hydrogen-bonded solvent molecule only when the solvent configuration brings the system to the crossing point according to Kuznetsov model.<sup>23–26</sup> In the model, the overall proton-transfer time is a sum of two times,  $\tau = \tau_1 + \tau_2$ , where  $\tau_1$  is the characteristic time for the solvent reorganization,  $\tau_S$ , and  $\tau_2$  is the time for the proton to pass to the acceptor molecule.

## Discussion

Abnormal proton mobility in water is traditionally thought to be governed by water molecule rotation. It is customary to subtract from the measured proton mobility a hydrodynamic part of  $H_3O^+$  motion, as estimated from water self-diffusion or as  $K^+$  mobility.<sup>14</sup> The difference, known as “prototropic” or abnormal protic mobility, represents the part due to a proton-transfer mechanism. The validity of this procedure has been questioned by Agmon.<sup>41</sup> He compared water rotation times with proton-hopping times, calculated with and without the subtraction of the hydrodynamic part (eqs 1 and 2). He concluded that the hydrodynamic proton mobility is considerably smaller than previously believed because the  $H_3O^+$  is nearly immobilized by extrastrong hydrogen bonds to first-shell water ligands, estimated to be about 8 kJ/mol stronger than bulk hydrogen bonds. From data analysis, he finds that water rotation is slower than proton hopping below 20 °C and has a hydrodynamic component to its activation energy. The proton mobility is not governed by water rotation as suggested by Bernal and Fowler<sup>10</sup> but rather by hydrogen-bond dynamics.

Voth and co-workers,<sup>42</sup> using an empirical valence bond (EVB) methodology, found statistically clear evidence of the proposed “Moses mechanism” for proton transport in liquid water. The mechanism suggests first a hydrogen-bond cleavage in the second solvation shell, which subsequently enables the exchange of a proton between the hydronium and a neighboring water molecule. Only after this transfer is a hydrogen-bond

formation observed on the proton-donor oxygen, as it returns to a more water-like environment.

Parinello and co-workers<sup>29–31</sup> looked at the nature of the hydrated excess proton in water using ab initio simulations. They found that the hydrated proton forms a defect in the hydrogen-bonded network with both  $H_9O_4^+$  and  $H_5O_2^+$  dimer structures and the rate of proton diffusion is determined by thermally induced hydrogen-bond breaking in the second solvation shell.

In this paper, we calculate the proton-transfer rate constant associated with the abnormal proton conductance in water (as deduced from eq 2) as a function of temperature and compare it with the corresponding values of the dielectric relaxation time,  $\tau_D$ . In our previous studies, we found that the temperature dependence of the proton-transfer rate constant from a photoacid to alcohols exhibits non-Arrhenius behavior. We found that, at low temperatures, the proton-transfer rate constant follows the inverse of  $\tau_D$ ,  $k_{PT} = b/\tau_D$ , where  $b$  is an empirical factor and its value for methanol is  $\sim 2$ . The abnormal proton conductance exhibits similar temperature dependence. For this reason, we used a similar approach to explain its peculiar temperature dependence in the current paper.

Conventional Landau–Zener (LZ) theory<sup>43,44</sup> provides an accurate description of the curve-crossing process in the absence of an interaction with the environment. It is applicable if the motion in the vicinity of the crossing point is nearly uniform (ballistic).<sup>45,46</sup> The interaction of the particle with the environment causes complications. Rips and Pollak<sup>47</sup> showed that variational transition-state theory (VTST) allows for the identification of a collective coordinate along which the dynamics in the curve-crossing region is maximally separated from the remaining solvent-induced dynamics (quasiballistic). The problem of calculation of the transition rate can then be handled using conventional LZ theory.

Our model calculations show that, at high temperatures (the nonadiabatic limit), the generalized water configuration motion is fast, the activation energy is sufficiently low, and the proton-tunneling rate is the rate-determining step. The LZ transmission coefficient is small and hence limits the rate of population transfer to the product (crossing to the product diabatic potential surface, see Figure 3). From the rate constant at high temperatures (the nonadiabatic limit, eq 7), we determine the preexponential factor and the activation energy of the process.

The preexponential factor is mainly determined by the value of the coupling matrix element. The transmission coefficient from the reactant well to the product well at the crossing point (at the top of the barrier) is given by the Landau–Zener transmission coefficient (eq 4). The adiabaticity parameter,  $\gamma$  (eqs 5a and 12), is determined by three parameters,  $|V|^2$ ,  $\Delta F$ , and  $\dot{S}$ .  $|V|^2$  can be evaluated from the experimental high-temperature rate constant. We find that the preexponential factor is  $1.2 \times 10^{12} \text{ s}^{-1}$ . From the preexponential expression, we evaluate  $V$  to be  $\sim 50 \text{ cm}^{-1}$  and  $(2\pi/\hbar)|V|^2 \cong 5 \times 10^{-8} \text{ J s}^{-1}$ .  $\Delta F = k_S$  where  $k_S$  is the mean force constant, which is related to the solvent reorganization energy,  $k_S = 2E_S$ . For water, we used the reorganization energy  $E_S = 0.3 \text{ eV}$ . To quantitatively evaluate the adiabaticity parameter,  $\gamma = \gamma'\tau_S$ , we calculate  $\gamma' = (2\pi/\hbar)|V|^2(1/\Delta F) \cong 2 \times 10^{11} \text{ s}^{-1}$ . We find that the calculated value of  $\gamma'$  is larger by about a factor of 4 than the value that we used to obtain the best fit to the experimental data in the actual calculation of the temperature dependence of the proton-transfer rate constant associated with the abnormal proton conductivity shown in Figures 2 and 4.

In our previous work,<sup>16</sup> we found for the proton-transfer rate from the super photoacid DCN2 to methanol or glycerol that,

at a low enough temperature (the solvent-controlled limit), the diffusive propagation of the solvent configuration toward the crossing region is slow compared to the tunneling rate. The LZ transmission coefficient is close to one because the average solvent velocity is slow (eq 5), and the rate-determining step is the transport motion of the probability density function of the solvent configuration itself, which appears also in the sink term (eq 14). The activation energy of the process,  $\Delta G^\ddagger$ , remains small but the diffusion constant (which is related to the average velocity of the solvent configuration) exhibits large temperature dependence. In the solvent-controlled limit rate expression (eq 10), the preexponential factor of the electron-transfer rate constant is determined by  $\tau_L$ . From our analysis and data fit, we find the average solvent velocity at the crossing point,  $\dot{S} = b/\tau_D$ , where  $b$  is an empirical factor.

From previous studies on alcohols and also in this study, we find that the solvent characteristic time for proton transfer,  $\tau_S = \tau_D/b$ , is in the range  $\tau_D > \tau_S > \tau_L$ , where  $\tau_L = (\epsilon_\infty/\epsilon_S)\tau_D$  is the longitudinal dielectric relaxation time. For methanol, we found the value of the empirical factor  $b \approx 2.1$ , and for the abnormal proton conductivity in water, we found a larger value,  $b = 9.2$ . The values of  $\tau_L$  for water and methanol can be estimated from the value of the low- and high-frequency dielectric constants of water and methanol,  $\epsilon_S$  and  $\epsilon_\infty$ , relevant for the proton-transfer process. The static dielectric constants of the two solvents are  $\epsilon_S^{\text{water}} = 78$  and  $\epsilon_S^{\text{MeOH}} = 32$  at 298 K. The description of the dielectric relaxation literature results for water requires a superposition of two Debye processes.<sup>48–50</sup> The high-frequency dielectric constant of the slower process is about  $\epsilon = 6.5$ , and the dielectric relaxation times range from  $\sim 6$  ps at 310 K to 18 ps at 273 K. The faster process that contributes the second Debye relaxation time is of about 1 ps, and its high-frequency dielectric constant is about 4.5. The ratio for the slow process,  $\epsilon_S/\epsilon_\infty$ , is 12, while we find from the fitting of the abnormal conductivity  $b = 9.2$ .  $\tau_L^{293\text{K}} = 0.8$  ps and  $\tau_S$  in our calculations is about 1.2 ps, about 50% longer than  $\tau_L$ . Garg and Smyth<sup>51</sup> found that the spectrum of dielectric relaxation of methanol shows three Debye dispersion regions. Jordan et al.<sup>52</sup> fitted their dielectric relaxation data for methanol employing the Cole–Cole distribution and found  $\epsilon_\infty^{\text{MeOH}} = 4.7$  at room temperature; the ratio  $\epsilon_S/\epsilon_\infty$  is 6.8. For DCN2 in methanol, we find  $b = 2.1$ . At 293 K,  $\tau_D^{\text{MeOH}} \approx 60$  ps,  $\tau_S^{\text{MeOH}} \approx 30$  ps, and  $\tau_L^{\text{MeOH}}$  is about 9 ps. The empirical factor,  $b$ , that we find by fitting the experimental data for proton transfer in water and methanol is somewhat smaller than the ratio  $\epsilon_S/\epsilon_\infty$ , which appears in the  $\tau_L$  definition.

In the calculation of the abnormal proton conductivity by the proton-transfer model based on the Landau–Zener curve-crossing formulation, we find that at 373 K, the boiling point of water, the reaction is in the nonadiabatic regime,  $\kappa_{LZ} = 0.01$ . At room temperature,  $\kappa_{LZ}$  increases slightly and is about 0.05, which means that the reaction is still in the nonadiabatic regime. The rate-limiting step is the proton motion, while the dynamics of the solvent configuration is fast and does not limit the rate of proton transfer. At 244 K, the adiabaticity parameter increases significantly,  $\gamma = 0.3$  and  $\kappa_{LZ} \approx 0.5$ . Thus, for supercooled water,  $T = 244$  K, the rate constant is determined by the dynamics of both coordinates, the solvent configuration and the proton tunneling. As discussed above in the case of proton transfer from DCN2 to alcohols,<sup>16</sup> we were able to observe a continuous transition from the nonadiabatic regime to the solvent-controlled limit by changing the temperature from high to low. In Figure 5, we also plot the Landau–Zener transmission coefficient as a function of  $1/T$  for our recent data<sup>16</sup> of the

proton-transfer reaction from DCN2 to methanol (squares). As seen,  $\kappa_{LZ}$  reaches the value of 1, the solvent-controlled limit, at about 170 K, close to the freezing point of methanol. For the proton transfer of DCN2 in glycerol, the midtransition point of the Landau–Zener transmission coefficient,  $\kappa_{LZ} = 0.5$ , occurred at 340 K while, for methanol, it occurred at 200 K. In the case of proton conductivity in an aqueous solution, even in the supercooled condition of 244 K, the reaction rate constant is mostly determined by the proton tunneling rate and the solvent dynamics limit the reaction rate to a lesser extent.

From our calculation, it arises that, up to about room temperature,  $\sim 290$  K, the abnormal conductivity is almost independent of the generalized solvent configuration motion because it is faster than the tunneling rate. Only at lower temperatures, solvent motion partially controls the proton-transfer process and the value of the rate constant is influenced by it. The fast proton-hopping time,  $\tau_p$  (1.5 ps at room temperature), slows at lower temperatures and is about 8 ps at 244 K. The experimental activation energy of the abnormal conductivity increases by a factor of approximately 5 because the relevant solvent motion that governs the proton-transfer process strongly depends on the temperature of supercooled water.

## Summary

Proton conductivity in aqueous solutions has been known for more than 150 years to be much larger than that of other cations. The abnormal proton conductivity in water arises from the efficient reaction of the proton transfer from  $\text{H}_3\text{O}^+$ , or larger hydrogen-bonded complexes such as  $\text{H}_9\text{O}_4^+$  (Eigen's complex)<sup>21</sup> or  $\text{H}_5\text{O}_2^+$  (the Zundel's dimer),<sup>22</sup> to a nearby water molecule or larger hydrogen-bonded complexes. Agmon<sup>11</sup> suggested that the molecular mechanism behind prototropic mobility involves a periodic series of isomerizations between  $\text{H}_9\text{O}_4^+$  and  $\text{H}_5\text{O}_2^+$ , the first triggered by hydrogen-bond cleavage of a second-shell water molecule and the second by the reverse hydrogen-bond formation process. In this study, we calculated the proton-transfer rate constant associated with prototropic mobility in water as a function of temperature. The prototropic mobility in aqueous solution exhibits non-Arrhenius behavior in the temperature range 240–373 K. At high temperature, the activation energy is small, while at low temperatures (at supercold water), it is large. We also found this behavior in the proton-transfer reaction from several photoacids to water and also in other protic solvents such as monols, diols, and glycerol. We found a strong correlation between the proton-transfer rate constant at low temperatures and the dielectric relaxation time,  $\tau_D$ . The model that we used to calculate the proton-transfer rate constant is based on diffusive propagation of the reactant population along a generalized solvent coordinate of the reactant potential surface toward the crossing point with the product potential surface. The proton transfer occurs at the crossing point, and the rate is calculated by a sink term placed at the crossing point. The sink term includes the solvent velocity and the Landau–Zener transmission coefficient,  $k_{LZ}$ , which depends on the adiabaticity parameter,  $\gamma$ . The adiabaticity parameter,  $\gamma$  (see eq 5), depends on three parameters, the difference between the reactant and product potential surfaces curvature ( $\Delta F$ ), the quantum tunneling coupling matrix element ( $|V|^2$ ), and the velocity of the generalized solvent coordinate in the vicinity of crossing ( $\dot{S}$ ).  $|V|^2$  is independent of temperature. The solvent velocity,  $\dot{S}$ , on the other hand, strongly depends on the temperature. In our previous papers,<sup>17–20</sup> we suggested that  $\dot{S}$  is related to the slow components of the solvent dielectric relaxation. We infer that

$\dot{S} = b/\tau_D$ , where  $\tau_D$  is the solvent dielectric relaxation time and  $b$  is an empirical factor, is dependent on the specific protic solvent. Both the diffusion constant and the Landau–Zener transmission coefficient depend on the dielectric relaxation of the solvent. The calculations are compared with the proton mobility data as a function of temperature. We find very good agreement between the calculation of the proton transfer rate associated with the prototropic mobility at all temperatures and the experimental measurements of proton conductivity as a function of temperature. The calculations indicate that at high water temperatures the rate-limiting step is proton tunneling while at low temperatures the solvent motion partially controls the proton-transfer rate.

**Acknowledgment.** We thank Prof. I. Rips and Prof. N. Agmon for their helpful discussion. This work was supported by grants from the US-Israel Binational Science Foundation and the James-Franck German-Israel Program in Laser-Matter Interaction.

## References and Notes

- (1) Conway, B. E. In *Modern Aspects of Electrochemistry*; Bockris, J. O'M., Conway, B. E., Eds.; Butterworths: London, 1964; Vol. 3.
- (2) Erdey-Gruz, T.; Lengyel, S. In *Modern Aspects of Electrochemistry*; Bockris, J. O'M., Conway, B. E., Eds.; Plenum Press: New York, 1977; Vol. 12.
- (3) Lengyel, S.; Conway, B. E. *Comprehensive Treatise of Electrochemistry*; Plenum Press: New York, 1983; Vol. 5, Chapter 4.
- (4) Agmon, N. *J. Phys. Chem.* **1996**, *100*, 1072. Errata: Agmon, N. *J. Phys. Chem.* **1997**, *101*, 4352.
- (5) Atkins, P. W. *Physical Chemistry*, 6th ed.; Oxford University Press: Oxford, U.K., 1998; Chapter 24.8, p 741.
- (6) de Grotthuss, C. J. T. *Ann. Chim.* **1806**, *LVIII*, 54.
- (7) Meiboom, S. *J. Chem. Phys.* **1961**, *34*, 375.
- (8) Halle, B.; Karlström, G. *J. Chem. Soc., Faraday Trans. 2* **1983**, *79*, 1031.
- (9) Pfeifer, R.; Hertz, H. G. *Ber. Bunsen-Ges. Phys. Chem.* **1990**, *94*, 1349.
- (10) Bernal, J. D.; Fowler, R. H. *J. Chem. Phys.* **1933**, *1*, 515.
- (11) Agmon, N. *Chem. Phys. Lett.* **1995**, *244*, 456.
- (12) Hasted, J. B. *Aqueous Dielectrics*; Chapman and Hall: London, 1973.
- (13) Simpson, J. H.; Carr, H. Y. *Phys. Rev.* **1958**, *111*, 1201.
- (14) Robinson, R. A.; Stokes, R. H. *Electrolyte Solutions*, 2nd ed.; Butterworth: London, 1959.
- (15) Cornish, B. D.; Speedy, R. J. *J. Phys. Chem.* **1984**, *88*, 1888.
- (16) Cohen, B.; Huppert, D. *J. Phys. Chem. A* **2002**, *106*, 7462.
- (17) Poles, E.; Cohen, B.; Huppert, D. *Isr. J. Chem.* **1999**, *39* (3–4), 347.
- (18) Cohen, B.; Huppert, D. *J. Phys. Chem. A* **2000**, *104*, 2663.
- (19) Cohen, B.; Huppert, D. *J. Phys. Chem. A* **2001**, *105*, 2980.
- (20) Cohen, B.; Huppert, D. *J. Phys. Chem. A* **2002**, *106*, 1946. Part of the special issue "Noboru Mataga Festschrift".
- (21) Eigen, M. *Angew. Chem., Int. Ed. Engl.* **1964**, *3*, 1.
- (22) Zundel, G.; Metzger, H. Z. *Phys. Chem. (N. F.)* **1968**, *58*, 225.
- (23) German, E. D.; Dogonadze, R. R.; Kuznetsov, A. M.; Levich, V. G.; Kharkats, Yu. I. *Elektrokhimiya* **1970**, *6*, 350.
- (24) German, E. D.; Kuznetsov, A. M.; Dogonadze, R. R. *J. Chem. Soc., Faraday Trans. 2* **1980**, *76*, 1128.
- (25) German, E. D.; Kuznetsov, A. M. *J. Chem. Soc., Faraday Trans. 1* **1981**, *77*, 397.
- (26) German, E. D.; Kuznetsov, A. M. *J. Chem. Soc., Faraday Trans. 2* **1981**, *77*, 2203.
- (27) Kuznetsov, A. M. *Charge Transfer in Physics, Chemistry and Biology*; Gordon and Breach, SA: Amsterdam, 1995.
- (28) Kreevoy, M. M.; Kotchevar, A. T. *J. Am. Chem. Soc.* **1990**, *112*, 3579. Kotchevar, A. T.; Kreevoy, M. M. *J. Phys. Chem.* **1991**, *95*, 10345.
- (29) Marx, D.; Tuckerman, M. E.; Hutter, J.; Parrinello, M. *Nature* **1999**, *397*, 604.
- (30) Tuckerman, M. E.; Laasonen, K.; Sprik, M.; Parrinello, M. *J. Chem. Phys.* **1995**, *103*, 150.
- (31) Tuckerman, M. E.; Laasonen, K.; Sprik, M.; Parrinello, M. *J. Phys. Chem.* **1995**, *99*, 5749.
- (32) Borgis, D.; Hynes, J. T. *J. Phys. Chem.* **1996**, *100*, 1118. Borgis, D. C.; Lee, S.; Hynes, J. T. *Chem. Phys. Lett.* **1989**, *162*, 19. Borgis, D.; Hynes, J. T. *J. Chem. Phys.* **1991**, *94*, 3619.
- (33) Hineman, M. F.; Brucker, G. A.; Kelley, D. F.; Bernstein E. R. *J. Chem. Phys.* **1992**, *97*, 3341.
- (34) Syage, J. A. *J. Phys. Chem.* **1995**, *99*, 5772.
- (35) Rips, I.; Jortner, J. *J. Chem. Phys.* **1987**, *87*, 2090.
- (36) Rips, I.; Jortner, J. In *Perspectives in Photosynthesis*; Jortner, J., Pullman, B., Eds.; Kluwer: Dordrecht, Netherlands, 1990; p 293.
- (37) Zusman, L. D. *Chem. Phys.* **1980**, *49*, 295.
- (38) Bicout, D. J.; Szabo, A. *J. Chem. Phys.* **1998**, *109*, 2325.
- (39) Agmon, N.; Hopfield, J. J. *J. Chem. Phys.* **1983**, *78*, 6947.
- (40) Krissinel', E. B.; Agmon, N. *J. Comput. Chem.* **1996**, *17*, 1085.
- (41) Agmon, N. *J. Chim. Phys. (Paris)* **1996**, *93*, 1714.
- (42) Day, T. J. F.; Schmitt, U. W.; Voth, G. A. *J. Am. Chem. Soc.* **2000**, *122*, 12027.
- (43) Landau, L. D. *Phys. Z. Sowjetunion* **1932**, *1*, 88; **1932**, *2*, 46.
- (44) Zener, C. *Proc. R. Soc. London, Ser. A* **1932**, *137*, 696.
- (45) Landau, L. D.; Lifshitz, E. M. *Quantum Mechanics: Nonrelativistic Theory*; Pergamon: New York, 1977; Section 90.
- (46) Nikitin, E. E.; Umanskii, S. Y. *Theory of Slow Atomic Collisions*; Springer: Berlin, 1984; Chapter 8.
- (47) Rips, I.; Pollak, E. *J. Chem. Phys.* **1995**, *103*, 7912.
- (48) Barthel, J.; Bachhuber, K.; Buchner, R.; Hetzenauer, H. *Chem. Phys. Lett.* **1990**, *165*, 369.
- (49) Barthel, J.; Bachhuber, K.; Buchner, R.; Gill, J. B.; Kleebauer, M. *Chem. Phys. Lett.* **1990**, *167*, 62.
- (50) Buchner, R.; Barthel, J. *J. Mol. Liq.* **1995**, *63*, 55.
- (51) Garg, S. K.; Smyth, C. P. *J. Phys. Chem.* **1965**, *69*, 1294.
- (52) Jordan, B. P.; Sheppard, R. J.; Szwarnowski, S. *J. Phys. D: Appl. Phys.* **1978**, *11*, 695.